

P-type conductivity in bulk $\text{Al}_x\text{Ga}_{1-x}\text{N}$ and $\text{Al}_x\text{Ga}_{1-x}\text{N}/\text{Al}_y\text{Ga}_{1-y}\text{N}$ superlattices with average Al mole fraction >20%

J. K. Kim, E. L. Waldron, Y.-L. Li, Th. Gessmann, and E. F. Schubert^{a)}

*Future Chips Constellation, Rensselaer Polytechnic Institute, Troy,
New York 12180*

H. W. Jang and J.-L. Lee

*Department of Materials Science and Engineering, Pohang University of Science and Technology, Pohang,
Kyungbuk 790-784, South Korea*

(Received 3 November 2003; accepted 3 March 2004)

Synchrotron radiation photoemission spectroscopy reveals enhanced oxygen incorporation in $\text{Al}_x\text{Ga}_{1-x}\text{N}$ as the Al mole fraction increases. It is shown that the increased oxygen donor incorporation can result in a conductivity-type change from p-type to n-type in Mg-doped $\text{Al}_x\text{Ga}_{1-x}\text{N}$. Consistent with the conductivity-type change, epitaxial $\text{Al}_{0.20}\text{Ga}_{0.80}\text{N}$ films exhibit n-type conductivity despite heavy Mg doping. The p-type conductivity of bulk $\text{Al}_x\text{Ga}_{1-x}\text{N}$ with a high Al mole fraction can be improved by employing $\text{Al}_x\text{Ga}_{1-x}\text{N}/\text{Al}_y\text{Ga}_{1-y}\text{N}$ superlattices (SLs). At 300 K, Mg-doped $\text{Al}_{0.17}\text{Ga}_{0.83}\text{N}/\text{Al}_{0.36}\text{Ga}_{0.64}\text{N}$ SLs (average Al mole fraction of 23%) exhibit strong p-type conductivity with a specific resistance of 4.6 $\Omega\text{ cm}$, a hole mobility of 18.8 cm^2/Vs , and an acceptor activation energy of 195 meV. © 2004 American Institute of Physics.

[DOI: 10.1063/1.1728322]

Highly conductive p-type $\text{Al}_x\text{Ga}_{1-x}\text{N}$ layers with high Al mole fraction x are of crucial importance for various electronic and optoelectronic devices including ultraviolet (UV) light-emitting diodes (LEDs). The attainment of p-type conductivity of Mg-doped $\text{Al}_x\text{Ga}_{1-x}\text{N}$, however, has been difficult due to a large acceptor activation energy of 150–250 meV as well as to a low hole mobility in heavily Mg-doped $\text{Al}_x\text{Ga}_{1-x}\text{N}$.^{1–4} The problem is particularly severe when $x > 20\%$. This is due to the increase of the acceptor activation energy and also due to an increase in unintentional donor concentration with increasing x . For high Al mole fractions, the O donor concentration could result in insulating or even n-type characteristics of $\text{Al}_x\text{Ga}_{1-x}\text{N}$ despite heavy Mg doping. Neither a theoretical calculation nor an experimental analysis of this compensation mechanism has yet been provided.

In order to improve p-type conductivity in bulk $\text{Al}_x\text{Ga}_{1-x}\text{N}$ films, Mg doped $\text{Al}_x\text{Ga}_{1-x}\text{N}/\text{GaN}$ superlattices (SLs) have been proposed⁵ and demonstrated to have excellent acceptor activation resulting in much lower resistivity.^{6–9} This concept can also be realized for high Al mole fractions by introducing “GaN-free” $\text{Al}_x\text{Ga}_{1-x}\text{N}/\text{Al}_y\text{Ga}_{1-y}\text{N}$ SLs rather than $\text{Al}_x\text{Ga}_{1-x}\text{N}/\text{GaN}$ SLs. Optical absorption at UV wavelengths is reduced in $\text{Al}_x\text{Ga}_{1-x}\text{N}/\text{Al}_y\text{Ga}_{1-y}\text{N}$ SLs as compared to that in $\text{Al}_x\text{Ga}_{1-x}\text{N}/\text{GaN}$ SLs, making the former type very attractive for UV LED and laser applications.

In this letter, it is shown that, in addition to the deepening of the acceptor energy, enhanced incorporation of O on substitutional N sites occurring at high Al mole fractions, as demonstrated by synchrotron radiation photoemission spectroscopy (SRPES), plays a crucial role in the conductivity-type change in bulk Mg-doped $\text{Al}_x\text{Ga}_{1-x}\text{N}$. In addition, the enhancements in hole concentration and mobility in

$\text{Al}_x\text{Ga}_{1-x}\text{N}/\text{Al}_y\text{Ga}_{1-y}\text{N}$ SLs are investigated using the Hall effect. It is shown that Mg-doped $\text{Al}_{0.17}\text{Ga}_{0.83}\text{N}/\text{Al}_{0.36}\text{Ga}_{0.64}\text{N}$ SLs show p-type conductivity, whereas uniformly doped $\text{Al}_{0.20}\text{Ga}_{0.80}\text{N}$ films show n-type conductivity despite heavy Mg doping.

The Mg-doped $\text{Al}_{0.17}\text{Ga}_{0.83}\text{N}/\text{Al}_{0.36}\text{Ga}_{0.64}\text{N}$ SLs were grown by metallorganic chemical vapor deposition (MOCVD) on c-plane sapphire. Undoped GaN buffer layers with a thickness of 1.5 μm were grown first, followed by the $\text{Al}_{0.17}\text{Ga}_{0.83}\text{N}/\text{Al}_{0.36}\text{Ga}_{0.64}\text{N}$ SLs doped with Mg. All doped regions have a Mg concentration of $N_{\text{Mg}} = 10^{19}\text{ cm}^{-3}$. The SLs have 20 periods, a barrier width of $L_B = 25\text{ \AA}$, and a well width of $L_W = 50\text{ \AA}$. The average Al mole fraction of the SLs is $(x_B L_B + x_W L_W)/(L_B + L_W) = 23\%$. Mg-doped bulk $\text{Al}_{0.20}\text{Ga}_{0.80}\text{N}$ was grown for comparison. Furthermore, bulk $\text{Al}_x\text{Ga}_{1-x}\text{N}$ films ($x = 0.0, 0.12, 0.22, 0.33$) were grown for SRPES analysis of O incorporation with increasing x . The Al mole fractions in the $\text{Al}_x\text{Ga}_{1-x}\text{N}$ films were determined by x-ray diffraction.

The variable temperature Hall-effect measurements were performed from 220 to 420 K in 10 K increments using the van der Pauw geometry. Pd/Au p-type Ohmic contacts were deposited using e-beam evaporation. A cryostat was used and the magnetic field was 0.5 T. The chemical bonding states at the surface of the $\text{Al}_x\text{Ga}_{1-x}\text{N}$ films were analyzed using SRPES at the Pohang Accelerator Laboratory in South Korea. The incident photon energy of 600 eV was used for obtaining Ga 3d, N 1s, Al 2p, and O 1s core level spectra.

The carrier concentration in $\text{Al}_x\text{Ga}_{1-x}\text{N}$ calculated as a function of Al mole fraction x is shown in Fig. 1. The free-hole concentration p in a partially compensated p-type semiconductor with acceptor concentration N_A , donor concentration N_D , and acceptor activation energy E_a is given by¹⁰

$$p = -\frac{N_D}{2} + \frac{N_D}{2} \left\{ 1 + 2 \left(\frac{N_A - N_D}{N_D^2} \right) N_V \times e^{-E_a/kT} \right\}^{1/2},$$

^{a)}Electronic mail: efschubert@rpi.edu

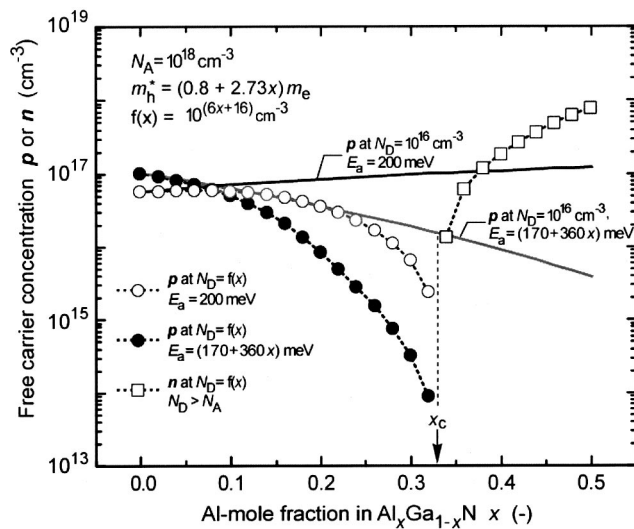


FIG. 1. Calculated hole concentration vs Al mole fraction x for p-type $\text{Al}_x\text{Ga}_{1-x}\text{N}$. The solid lines represent the hole concentration when $N_D = 1 \times 10^{16} \text{ cm}^{-3}$, and $E_a = 200$ and $(170 + 360x)$ meV, respectively. The open and solid circles represent the hole concentration when $N_D = 10^{(6x+16)} \text{ cm}^{-3}$, $E_a = 200$ and $(170 + 360x)$ meV, respectively. The squares represent the free electron concentration when the N_D exceeds N_A .

where N_v is the effective density of states at the valence band edge. In the calculation, we assume $T = 300 \text{ K}$, $N_A = 1 \times 10^{18} \text{ cm}^{-3}$, and $E_a = (170 + 360x)$ meV, which is the average of several values reported in the literature.^{11–13} For calculating N_v , we estimate $m_h^* = (0.8 + 2.7x)m_e$ for $\text{Al}_x\text{Ga}_{1-x}\text{N}$ by a linear extrapolation of $m_h^* = 3.5m_e$ for AlN and $m_h^* = 0.8m_e$ for GaN.¹⁴ Assuming that the background donor concentration is independent of x ($N_D = 1 \times 10^{16} \text{ cm}^{-3}$), the p decreases with increasing x . The p slightly increases when $E_a = 200$ meV due to the increase in m_h^* and N_v , as shown by the solid lines in Fig. 1. This indicates that the attainment of high hole concentrations in $\text{Al}_x\text{Ga}_{1-x}\text{N}$ is difficult due to the deepening of acceptor energy with increasing x . An additional factor is the increase in the concentration of compensating O donors with increasing x . Linear interpolation of $N_D = 1 \times 10^{16} \text{ cm}^{-3}$ at $x = 0$ and $N_D = 1 \times 10^{19} \text{ cm}^{-3}$ at $x = 0.5$ (Ref. 15) yields a donor concentration dependence on x of $N_D = 10^{(6x+16)} \text{ cm}^{-3}$. As a result, the p decrease rapidly with increasing x , as shown by open circles [$E_a = 200$ meV] and solid circles [$E_a = (170 + 360x)$ meV] in Fig. 1. This indicates an additional impediment to p-type conductivity in $\text{Al}_x\text{Ga}_{1-x}\text{N}$. Furthermore, when $N_D > N_A$ at x_c , the film exhibits n-type conductivity, as shown by squares in Fig. 1.

Figure 2 displays the relative ratio of bond intensity and the relative O concentration in $\text{Al}_x\text{Ga}_{1-x}\text{N}$ as a function of Al mole fraction measured by SRPES. The bond intensity is the integrated intensity of each chemical bond, extracted from the spectral deconvolutions of the Ga $3d$ and the Al $2p$ spectra. The core level spectra have been decomposed into spectral components corresponding to possible bonding states of the elements which give rise to different chemical shifts of the core level spectra. The spectral line shape was simulated with a suitable combination of the Voigt line shapes possessing a Gaussian broadening function which give the best fit of the spectra. The relative atomic concentration of O in $\text{Al}_x\text{Ga}_{1-x}\text{N}$ was determined from the inter-

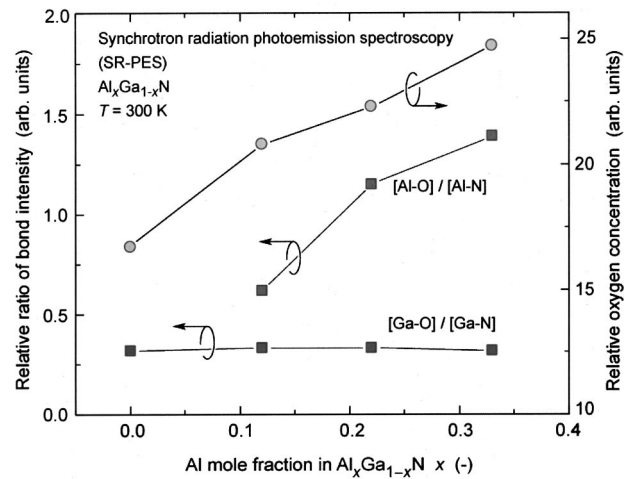


FIG. 2. Relative ratio of bond intensity $[\text{Al-O}]/[\text{Al-N}]$ and $[\text{Ga-O}]/[\text{Ga-N}]$ vs Al mole fraction x for $\text{Al}_x\text{Ga}_{1-x}\text{N}$, measured by SRPES. Also shown is a relative O concentration vs Al mole fraction.

grated intensities of Ga $3d$, Al $2p$, N $1s$, and O $1s$ spectra considering the atomic sensitivity factors of each element.¹⁶ The relative ratio of $[\text{Ga-O}]/[\text{Ga-N}]$ intensity is almost the same independent of x . On the other hand, the relative ratio of $[\text{Al-O}]/[\text{Al-N}]$ intensity and the O concentration increase simultaneously with x . This provides clear and strong evidence that the incorporation of O atoms with Al is enhanced with increasing x by occupying substitutional N sites. Oxygen is an omnipresent impurity in the $\text{Al}_x\text{Ga}_{1-x}\text{N}$ material system and it has been reported to be responsible for the background electron concentration.¹⁷ In $\text{Al}_x\text{Ga}_{1-x}\text{N}$, it has been reported that O atoms occupying N sites, O_N , act as shallow donors.¹⁷ In addition, Al has strong affinity for O. Therefore, the background electron concentration in $\text{Al}_x\text{Ga}_{1-x}\text{N}$ increases due to the enhanced incorporation of O donors with increasing x . As a result, a high degree of compensation or even a conductivity-type conversion, as shown in Fig. 1, is expected in Mg-doped $\text{Al}_x\text{Ga}_{1-x}\text{N}$ with high x .

Consistent with this prediction, a bulk $\text{Al}_{0.20}\text{Ga}_{0.80}\text{N}$ film exhibits n-type conductivity despite Mg concentration as high as $N_{\text{Mg}} = 10^{19} \text{ cm}^{-3}$. The free electron concentration and mobility of the $\text{Al}_{0.20}\text{Ga}_{0.80}\text{N}$ film were $2.4 \times 10^{16} \text{ cm}^{-3}$ and $55.9 \text{ cm}^2/\text{Vs}$, respectively. On the other hand, the Mg-doped $\text{Al}_{0.17}\text{Ga}_{0.83}\text{N}/\text{Al}_{0.36}\text{Ga}_{0.64}\text{N}$ SL sample shows p-type conductivity, despite average x as high as 23%. Figure 3 shows the hole concentration and hole mobility of the Mg-doped $\text{Al}_{0.17}\text{Ga}_{0.83}\text{N}/\text{Al}_{0.36}\text{Ga}_{0.64}\text{N}$ SL sample as a function of reciprocal temperature. The mobility decreases monotonically with increasing temperature due to a combination of phonon scattering and piezoelectric scattering. The hole mobility at 300 K is $18.8 \text{ cm}^2/\text{Vs}$. This hole mobility is comparable to the values ($19 \text{ cm}^2/\text{Vs}$) reported for $\text{Al}_x\text{Ga}_{1-x}\text{N}/\text{GaN}$ SL grown by molecular beam epitaxy,⁶ and higher than the values ($< 10 \text{ cm}^2/\text{Vs}$) for $\text{Al}_x\text{Ga}_{1-x}\text{N}/\text{GaN}$ SLs grown by MOCVD.^{7,12} An effective acceptor activation energy E_a is extracted from a linear fit of p vs. $1/T$. The acceptor activation energy is determined to be 195 meV, much smaller than that of bulk $\text{Al}_{0.23}\text{Ga}_{0.77}\text{N}$, which is 253 meV, as calculated from $E_a = (170 + 360x)$ meV.^{11–13}

The resistivity of the $\text{Al}_{0.17}\text{Ga}_{0.83}\text{N}/\text{Al}_{0.36}\text{Ga}_{0.64}\text{N}$ SL

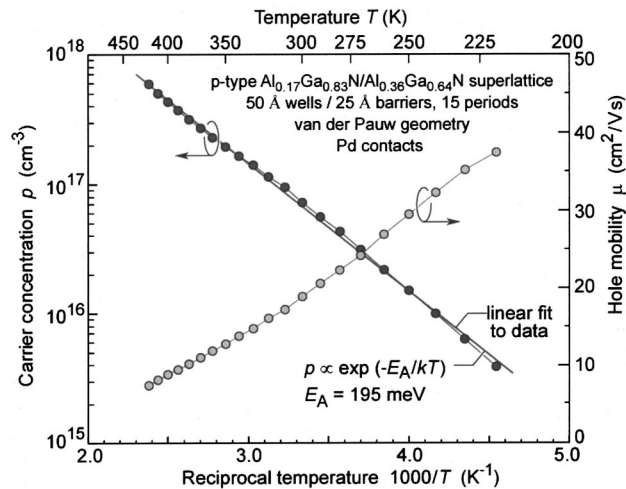


FIG. 3. Variable temperature three-dimensional carrier concentration and hole mobility of Mg-doped $\text{Al}_{0.17}\text{Ga}_{0.83}\text{N}/\text{Al}_{0.36}\text{Ga}_{0.64}\text{N}$ SL. The straight line represents a linear fit to the carrier concentration giving an acceptor activation energy of 195 meV.

sample as a function of temperature is shown in Fig. 4. The resistivities at 300 and 400 K are 4.6 and 1.5 $\Omega\text{ cm}$, respectively. Compared to the Mg-doped bulk $\text{Al}_{0.07}\text{Ga}_{0.93}\text{N}$,⁹ the $\text{Al}_{0.17}\text{Ga}_{0.83}\text{N}/\text{Al}_{0.36}\text{Ga}_{0.64}\text{N}$ SL shows a much smaller resistivity despite a three times higher average x . As originally proposed by Schubert *et al.*,^{5,12} SLs increase the overall hole concentration by allowing deep acceptors in the barriers to ionize into the valence band of the neighboring narrow-bandgap materials. In addition, piezoelectric coefficients for GaN-based materials are about one order of magnitude higher than other III-V semiconductors, leading to huge electric fields.⁶ This large polarization field creates a periodic sawtooth-shaped variation in the band edges which results in a periodic lowering of the acceptor level below the Fermi level, thus creating sheet carriers at each interface, as shown in the inset of Fig. 4. Furthermore, as x increases, the strain-induced piezoelectric field will increase, which in turn helps achieve higher hole concentrations. The increase of O contents with increasing x seems to affect both the bulk $\text{Al}_x\text{Ga}_{1-x}\text{N}$ and $\text{Al}_x\text{Ga}_{1-x}\text{N}/\text{Al}_y\text{Ga}_{1-y}\text{N}$ SL but the compensation of holes should be less in the $\text{Al}_x\text{Ga}_{1-x}\text{N}/\text{Al}_y\text{Ga}_{1-y}\text{N}$ SL. In comparison with $\text{Al}_x\text{Ga}_{1-x}\text{N}/\text{GaN}$ SLs, the $\text{Al}_x\text{Ga}_{1-x}\text{N}/\text{Al}_y\text{Ga}_{1-y}\text{N}$ SLs exhibit high p-type conductivity even for high average Al mole fractions. The reduced optical absorption effects at a short wavelength range make the $\text{Al}_x\text{Ga}_{1-x}\text{N}/\text{Al}_y\text{Ga}_{1-y}\text{N}$ SLs very attractive for UV device applications.

In summary, a high degree of compensation or even a p-type-to-n-type conductivity-type conversion in bulk $\text{Al}_x\text{Ga}_{1-x}\text{N}$ is concluded to occur due to the enhanced incorporation of donor impurities. SRPES measurements on bulk $\text{Al}_x\text{Ga}_{1-x}\text{N}$ indicate that the incorporation of O atoms into substitutional N sites is enhanced with increasing x , leading to an increase in background electron concentration, N_D . Consistent with these findings, epitaxial $\text{Al}_{0.20}\text{Ga}_{0.80}\text{N}$ films are found to exhibit n-type conductivity despite heavy Mg doping. The lack of p-type conductivity is overcome by employing $\text{Al}_x\text{Ga}_{1-x}\text{N}/\text{Al}_y\text{Ga}_{1-y}\text{N}$ SLs. Mg-doped $\text{Al}_{0.17}\text{Ga}_{0.83}\text{N}/\text{Al}_{0.36}\text{Ga}_{0.64}\text{N}$ SLs with average x of 23% ex-

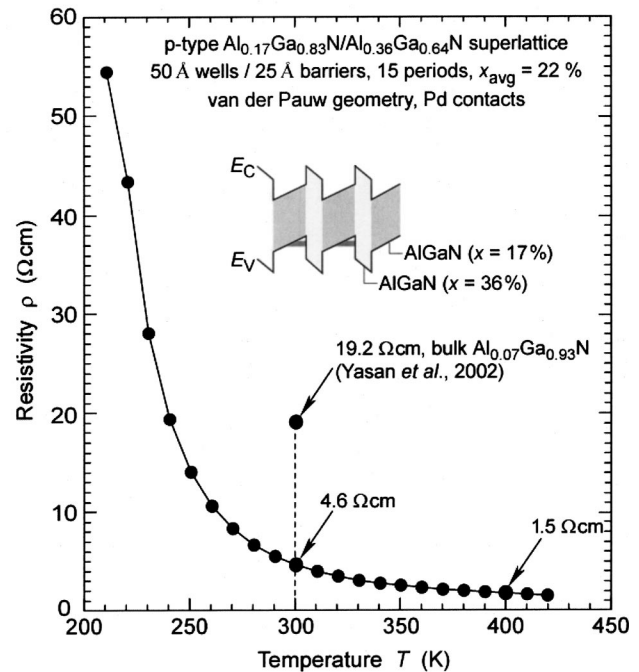


FIG. 4. Variable temperature resistivity of Mg-doped $\text{Al}_{0.17}\text{Ga}_{0.83}\text{N}/\text{Al}_{0.36}\text{Ga}_{0.64}\text{N}$ SL. The inset shows schematic energy band diagram of $\text{Al}_{0.17}\text{Ga}_{0.83}\text{N}/\text{Al}_{0.36}\text{Ga}_{0.64}\text{N}$ SL with internal polarization fields.

hibit strong p-type conductivity with resistivity of 4.6 $\Omega\text{ cm}$ and mobility of 18.8 cm^2/Vs at 300 K. In addition, the E_a is calculated to be 195 meV, much lower than that of Mg-doped bulk $\text{Al}_{0.23}\text{Ga}_{0.77}\text{N}$, 250 meV.

This work was supported in part by the ONR/Univ. New Mexico, and DARPA/ARO.

- ¹H. Morkoç and S. Strite, *J. Vac. Sci. Technol. B* **10**, 1237 (1992).
- ²I. D. Goepfert, E. F. Schubert, A. Osinsky, and P. E. Norris, *Electron. Lett.* **35**, 1109 (1999).
- ³W. Götz, N. M. Johnson, J. Walker, D. P. Bour, and R. A. Street, *Appl. Phys. Lett.* **68**, 667 (1996).
- ⁴C. J. Eiting, P. A. Grudowski, and R. D. Dupuis, *Electron. Lett.* **33**, 1987 (1997).
- ⁵E. F. Schubert, W. Grieshaber, and I. D. Goepfert, *Appl. Phys. Lett.* **69**, 3737 (1996).
- ⁶P. Kozodoy, Y. P. Smorchkova, M. Hansen, H. Xing, S. P. DenBaars, U. K. Mishra, A. W. Saxler, R. Perrin, and W. C. Mitchel, *Appl. Phys. Lett.* **75**, 2444 (1999).
- ⁷P. Kozodoy, M. Hansen, S. P. DenBaars, and U. K. Mishra, *Appl. Phys. Lett.* **74**, 3681 (1999).
- ⁸E. L. Waldron, J. W. Graff, and E. F. Schubert, *Appl. Phys. Lett.* **79**, 2737 (2001).
- ⁹A. Yasan, R. McClintock, S. R. Darvish, Z. Lin, K. Mi, P. Kung, and M. Razeghi, *Appl. Phys. Lett.* **80**, 2108 (2002).
- ¹⁰E. F. Schubert, *Doping in III-V Semiconductors* (Cambridge University Press, Cambridge, United Kingdom, 1993), p. 130.
- ¹¹M. G. Cheong, K. S. Kim, C. S. Kim, R. J. Choi, H. S. Yoon, N. W. Namgung, E.-K. Suh, and H. J. Lee, *Appl. Phys. Lett.* **80**, 1001 (2002).
- ¹²I. D. Goepfert, E. F. Schubert, A. Osinsky, P. E. Norris, and N. N. Faleev, *J. Appl. Phys.* **88**, 2030 (2000).
- ¹³T. Tanaka, A. Watanabe, A. Amano, Y. Kobayashi, I. Akasaki, S. Yamazaki, and M. Koike, *Appl. Phys. Lett.* **65**, 593 (1994).
- ¹⁴M. N. Yoder, *Proc. SPIE* **CR45**, 105 (1993).
- ¹⁵M. D. McCluskey, N. M. Johnson, C. G. Van de Walle, D. P. Bour, and M. Kneissl, *Phys. Rev. Lett.* **80**, 4008 (1998).
- ¹⁶J. F. Moulder, W. F. Stickle, P. E. Sobol, and K. D. Bomben, *Handbook of X-ray Photoelectron Spectroscopy* (Perkin-Elmer Corp., Eden Prairie, MN, 1992).
- ¹⁷W. Götz, J. Walker, L. T. Romano, and N. M. Johnson, *Proc. Mater. Res. Soc.* **449**, 525 (1997).